Carbohydrate Polymers 340 (2024) 122310

Contents lists available at ScienceDirect

Carbohydrate Polymers

journal homepage: www.elsevier.com/locate/carbpol

Electrodeposition of cellulose nanofibers as an efficient dehydration method

Takaaki Kasuga [*,1], Chenyang Li [1], Ami Mizui, Shun Ishioka, Hirotaka Koga, Masaya Nogi

SANKEN (The Institute of Scientific and Industrial Research), Osaka University, Ibaraki, Osaka 567-0047, Japan

ARTICLE INFO

Keywords:
Cellulose nanofibers
Nanocellulose
Electrodeposition
Dehydration
Transparent film

ABSTRACT

Dehydration of a cellulose nanofiber (CNF)/water dispersion requires large amounts of energy and time due to the high hydrophilicities and high specific surface areas of the CNFs. Various dehydration methods have been proposed for CNF/water dispersions; however, an efficient dehydration method for individually dispersed CNFs is needed. Here, electrodeposition of CNFs was evaluated as a dehydration method. Electrodeposition at a DC voltage of 10 V on a 0.2 wt% CNF/water dispersion resulted in a concentration of ~1.58 wt% in 1 h. The dehydration energy efficiency was ~300 times greater than that of dehydration by evaporation. The concentrated CNF hydrogels recovered after electrodeposition were redispersed with a simple neutralization process, and clear transparent films were obtained by drying after redispersion. This work provides a new method for dehydration and reuse of individually dispersed CNF/water dispersions and provides new insights into control of the hierarchical structures of CNFs by electrodeposition.

1. Introduction

Cellulose nanofibers (CNFs) have attracted much attention as sustainable nanomaterials due to their excellent properties, such as mechanical strength, transparency, thermal resistance, high surface area, and biodegradability (Abe, Iwamoto, & Yano, 2007; Isogai, Saito, & Fukuzumi, 2011; Yang, Reid, Olsén, & Berglund, 2020). Various application studies with CNFs, including films, filters, hydrogels, aerogels, electronic substrates, and composites, have been reported (Huang, Kasuga, Nogi, & Koga, 2023; Kasuga, Mizui, Koga, & Nogi, 2023; Kasuga, Yagyu, Uetani, Koga, & Nogi, 2019; Li, Hatakeyama, & Kitaoka, 2022; Nemoto, Saito, & Isogai, 2015; Sakuma et al., 2021; Sakuma, Fujisawa, Berglund, & Saito, 2021; Zhu et al., 2022). CNFs are sustainable functional nanomaterials and are expected to be used as alternatives to petroleum-derived materials. In recent years, industrial production of CNFs has increased, especially in Japan, and CNF production facilities are being expanded for mass production. To achieve mass production and mass use of CNFs, it is important to consider the entire life cycle, including the production process and the transportation and storage costs.

CNFs are typically prepared from wood pulp via aqueous fibrillation (Abe et al., 2007; Isogai et al., 2011; Yang et al., 2020). CNF/water dispersions have high viscosity even at low concentrations (Lasseuguette, Roux, & Nishiyama, 2008), therefore, after preparation, the dispersions contain a large amount of water for effective fibrillation and homogenization. To reduce the transportation and storage costs, removal of large amounts of water from the CNF/water dispersions is necessary (Isobe, Kasuga, & Nogi, 2018; Kasuga, Isobe, Yagyu, Koga, & Nogi, 2018; Li, Kasuga, Uetani, Koga, & Nogi, 2020; Sinquefield, Ciesielski, Li, Gardner, & Ozcan, 2020; Yagyu et al., 2023). CNFs, which are hydrophilic nanofibers, have a high affinity for water and a high surface area (Abe et al., 2007; Isogai et al., 2011; Yang et al., 2020); therefore, the removal of water from CNF/water dispersions requires enormous amounts of energy and time. Various approaches have been explored for dehydration of CNF/water dispersions, including filtration, evaporation, osmotic concentration, freeze–thaw cycling, and centrifugation (Guccini et al., 2018; Sekine et al., 2020; Sheng & Yang, 2019; Sinquefield et al., 2020; Zhai, Kim, Kim, & Kim, 2020; Zhao et al., 2017). Vacuum filtration is a commonly used technique for dehydration of CNF/water dispersions. However, filtration is very time consuming because independently dispersed CNFs, such as 2,2,6,6-tetramethylpiperidine-1-oxylradical (TEMPO)-oxidized CNFs, form a fine network structure on the filter, preventing dehydration. For example, if a 0.2 wt% CNF/water dispersion was dehydrated by filtration, only 52.5 % water was

* Corresponding author.
E-mail address: tkasuga@eco.sanken.osaka-u.ac.jp (T. Kasuga).
[1] These authors contributed equally to this work

https://doi.org/10.1016/j.carbpol.2024.122310
Received 6 March 2024; Received in revised form 20 May 2024; Accepted 21 May 2024
Available online 22 May 2024

dehydrated after 24 h (Fig. S1). Evaporation such as a cast drying method and using a rotary evaporator can dehydrate faster than filtration with higher energy consumption due to the heat of evaporation. Currently, there are two options: fast dehydration with high energy consumption (e.g., evaporation) or low energy consumption for a long time (e.g., filtration, osmotic dewatering). It is not easy to achieve both high-speed dehydration and high energy efficiency.

Electrodeposition of nanocellulose, including CNFs, has attracted much attention in recent years (Guo et al., 2020; Kasuga, Saito, Koga, & Nogi, 2022; Kasuga, Yagyu, Uetani, Koga, & Nogi, 2021; Kim, Endrödi, Salazar-Alvarez, & Cornell, 2019; Wilson et al., 2018). CNFs dispersed in water are negatively charged (Isogai et al., 2011). When a DC voltage is applied to a CNF/water dispersion, the CNFs are deposited on the anode by electrodeposition (Guo et al., 2020; Kasuga et al., 2021; Kasuga et al., 2022; Kim et al., 2019; Wilson et al., 2018). The deposited CNFs form a hydrogel that is several times more concentrated than the dispersion due to electroosmosis (Karna, Lidén, Wohlert, & Theliander, 2021; Kasuga et al., 2022; Wetterling, Sahlin, Mattsson, Westman, & Theliander, 2018). Electrodeposition is a potential efficient dehydration method because it does not require water evaporation, which generates energy losses. However, the dehydration efficiency of electrodeposition for independently dispersed CNF/water dispersions, which are the most difficult to dehydrate, is still unclear. When CNFs are deposited electrophoretically, electrochemical reactions on the anode surface convert the counterions of the CNFs (Guo et al., 2020; Kasuga et al., 2021; Kasuga et al., 2022; Kim et al., 2019). It has also been suggested that there may be inhomogeneous cross-linking between CNFs during hydrogel formation on the anode (Kasuga et al., 2022). Uncontrolled orientations and cross-linking of CNFs limit their use after dehydration (Isobe et al., 2018; Kasuga et al., 2018). Therefore, the structural and chemical states of CNFs during electrodeposition should be evaluated in detail. In addition, it is necessary to determine reuse of the concentrated CNF hydrogels after electrodeposition.

Herein, we evaluated the electrodeposition of CNFs as a dehydration method. We focused on the dehydration efficiency and the chemical and structural characteristics of the concentrated CNF hydrogels at the anode. In addition, a process for preparing transparent nanopapers from concentrated CNF hydrogels formed on an anode was investigated.

2. Materials and methods

2.1. Preparation of CNF/water dispersions

TEMPO-oxidized cellulose pulp (carboxylate content: 1.8 mmol/g) was supplied by DKS Co., Ltd. The 0.5 wt% TEMPO-oxidized cellulose pulp slurry was homogenized using a high-pressure water-jet system (HJP-25008, Sugino Machine Co., Ltd., Japan) equipped with a ball-collision chamber. The slurry was repeatedly passed through a small nozzle (diameter: 0.15 mm) under a pressure of 200 MPa. The resulting dispersion was adjusted to a concentration of 0.2 wt% for subsequent use.

2.2. Electrodeposition

Two 10 × 10 × 0.5 cm graphite electrodes were placed in an acrylic cell (with a distance of 3 cm between the electrodes), and the cell was filled with 2 L of a 0.2 wt% CNF/water dispersion. Voltages ranging from 1 to 10 V were applied with a source measurement unit (B2902A, Keysight Technologies, USA). The CNF/water dispersion maintained the ambient temperature (~25 °C) throughout the entire voltage treatment. The concentration of the formed CNF hydrogel was quantified by drying at 110 °C. Voltages of 2.5, 5, and 10 V were required for 1, 3, and 6 h, respectively, to grow each hydrogel to a thickness of 5 mm. Squares (20 × 20 mm) were collected from the centers of the formed CNF hydrogels and used for structural characterization. Fourier Transform Infrared (FT-IR) spectra of CNF films prepared by drying the CNF hydrogels was obtained with an FT-IR spectrometer (Frontier TN, PerkinElmer Inc., USA). The cross-sections of the CNF hydrogels were observed through a cross-sectional polarized optical microscope (ECLIPSE LV100N POL, Nikon Corp., Japan).

2.3. Reusability test

CNF hydrogels prepared with a voltage of 10 V and a deposition time of 1 h were used for the reusability tests. For redispersion, the CNF hydrogels were simply homogenized at 8000 rpm for 10 min with a homogenizing mixer (MARKII Model 2.5, PRIMIX Corp., Japan) and diluted to 0.2 wt%. For neutralization, a 0.1 M sodium hydroxide solution was added to the redispersed CNF dispersion until the pH of the dispersion reached 7. The original, redispersed, and neutralized CNF/water dispersions were then cast-dried at 10 °C and 90 % RH to prepare CNF films (film thicknesses of ~18 μm). The total light transmittances of the CNF/water dispersions and CNF films were measured with a UV–vis-NIR spectrophotometer (UV-3600 Plus, Shimadzu Corp., Japan). The hazes and total transmittances of the CNF films were measured with a haze meter (NDH 8000, Nihon Dempa Kogyo Co., Ltd., Tokyo, Japan). The surface roughnesses were determined with a laser microscope (VK-X3000, Keyence Corp., Japan).

3. Results

3.1. Dehydration of CNF/water dispersions by electrodeposition

A 0.2 wt% TEMPO-oxidized CNF/water dispersion was used as the dehydrating target. The graphite electrodes were placed 3 cm from each other in a CNF/water dispersion, and DC voltages ranging from 1 to 10 V were applied between the electrodes. The CNF hydrogels formed on the anode were collected, and the CNF concentrations of the hydrogels were measured (Fig. 1a-c). When 1 V was applied, no CNF hydrogel formed on the anode, and the concentration of the CNF/water dispersion near the anode remained the same as the initial concentration (Fig. 1c). When 2.5–10 V was applied, CNF hydrogels were formed on the anode (Fig. 1c), and the CNF concentrations of the CNF hydrogels increased beyond the initial concentration (0.2 wt%). When 10 V was applied between the electrodes, CNF hydrogels with CNF concentrations of ~1.58 wt% were formed on the anode after 1 h, which was approximately 8 times more concentrated than the initial concentration. The concentrations of the deposited CNF hydrogels increased slowly as the electrodeposition time was extended beyond 1 h (Fig. 1c). During electrodeposition, deposition of the CNFs at the anode and concentration via electroosmosis proceed simultaneously (Guo et al., 2020; Kasuga et al., 2021; Kasuga et al., 2022; Kim et al., 2019). Therefore, even if the electrodeposition time was extended, the overall concentration of the CNF hydrogel did not increase substantially. The CNF concentration after electrodeposition for 1 h at different voltages linearly increased with the rise in the applied voltage (Fig. S2). These results suggested that repeated short-term electrodeposition at high voltage and collection of the deposited CNF hydrogel was more effective than long-term electrodeposition.

3.2. Comparison of the dehydration energy efficiencies for evaporation and electrodeposition

The energy consumed in dehydrating 1 g of water was calculated based on the amount of deposited CNFs, the CNF concentration and the energy consumption (Table S1). As a result, the energy consumption was ~0.0021 [Wh/g] when 10 V was applied for 1 h. The vaporization energy of water (~0.63 [Wh/g], @ 100 °C) was used for comparison (Wetterling et al., 2018). These results suggested that electrodeposition dehydrated the CNF/water dispersions ~300 times more efficiently than evaporation (Fig. 2). When electrodeposition (@ 10 V) was used to dehydrate a 0.2 wt% CNF/water dispersion, ~87 % of the water was

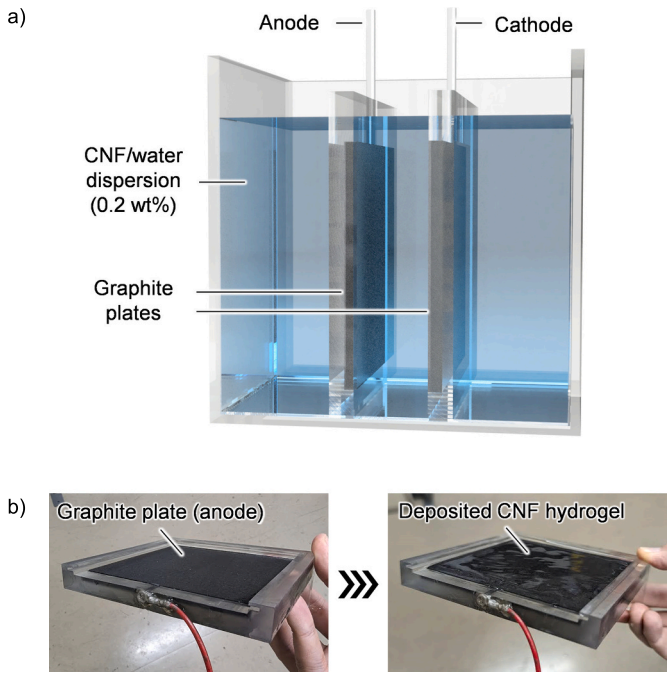

Fig. 1. a) Overview of the electrodeposition system. b) CNF hydrogels were formed on the anode by electrodeposition. c) Relationships between the applied voltages, application times and CNF concentrations of CNF hydrogels prepared by electrodeposition.

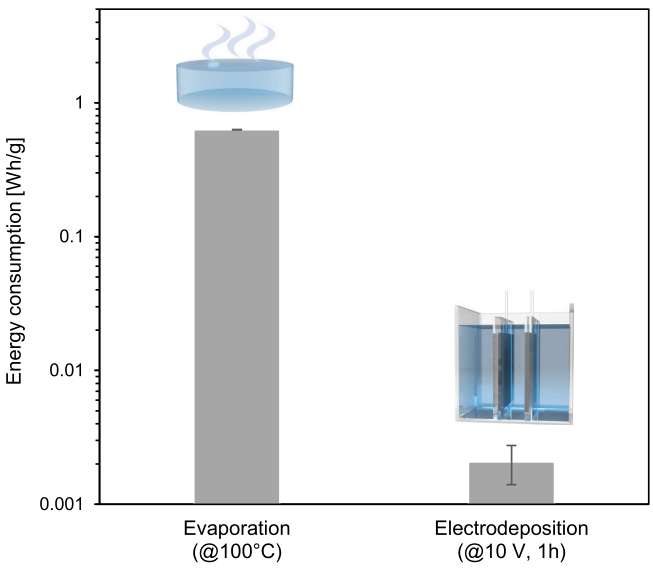

Fig. 2. Comparison of the dehydration energy consumed by evaporation and electrodeposition.

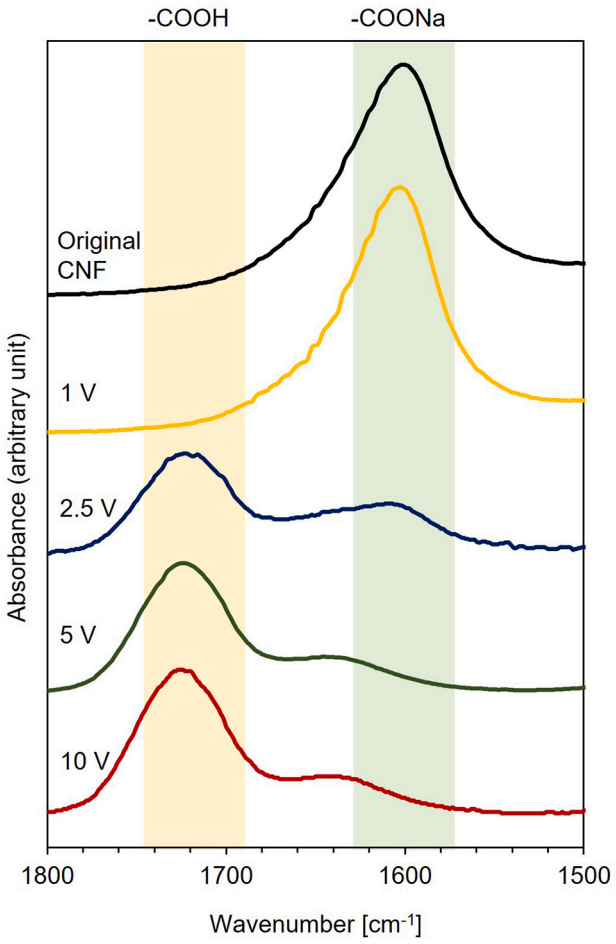

Fig. 3. FTIR spectra of the deposited CNFs after 1 h with different applied voltages.

removed in 1 h with high energy efficiency, making this a promising dehydration method for individually dispersed CNFs such as TEMPO-oxidized CNFs.

3.3. Counterion exchange of CNFs by electrodeposition

During electrodeposition at applied voltages of 2.5 V, 5 V and 10 V, the Na counterions (-COONa) of the CNFs were almost completely replaced with H (-COOH) (Fig. 3) (Shimizu, Saito, & Isogai, 2016; Sone, Saito, & Isogai, 2016). Protonation of the carboxy groups occurred because of the low pH around the anode caused by water electrolysis (Guo et al., 2020; Kasuga et al., 2021; Kasuga et al., 2022; Kim et al., 2019,). The initial pH of the CNF/water dispersion was ~6.8. After electrodeposition at 10 V for 1 h, the pH of the dispersion increased to ~10.7. The pH change was caused by water electrolysis and ion-exchange of protons (H^+) with the counter ion of carboxylate groups of CNFs (Na^+). It is thought that the hydroxide ions (OH^-) produced at the cathode became more abundant relative to protons (H^+) by the ion-

exchange, resulting in an increase in pH. In the case of electrodeposition at 2.5 V, a peak was observed that appeared to be from the residual sodium carboxylate groups (-COONa). This implied that some Na-type CNFs were not immediately converted to H-type CNFs during electrodeposition in the mild water electrolysis reactions. CNF hydrogels were not formed by electrodeposition at 1 V, and the Na counterions of the CNFs near the anode remained (Fig. 3). It has been reported that CNF hydrogels were formed even at an applied voltage of 1 V when copper was used as the anode (Kasuga et al., 2022). In this study, a graphite electrode was used as the anode, and no hydrogel was formed at an applied voltage of 1 V. With a copper electrode, CNF hydrogel formation was possible because the CNFs were cross-linked and fixed by the copper ions dissolved from the anode (Kasuga et al., 2022). On the other hand, in the case of the graphite anode, supply of cations for hydrogel formation did not occur; therefore, water electrolysis was essential for hydrogel formation.

3.4. Structural effects of electrodeposition on deposited CNF hydrogels

The structural characteristics of the deposited CNF hydrogels were then evaluated. The hydrogel deposited at 2.5 V had a clear appearance with no bubbles and a smooth surface (Fig. 4 a, b). On the other hand, the CNF hydrogels deposited at 5 V and 10 V had translucent appearances containing bubbles, and the gel surfaces were not smooth (Fig. 4c-f). The bubbles were most likely generated at the anode during the water electrolysis (Guo et al., 2020; Kasuga et al., 2021; Kasuga et al., 2022; Kim et al., 2019). At an applied voltage of 2.5 V, the water electrolysis was milder than those at 5 V and 10 V, suggesting that the oxygen diffused into the water before the bubbles grew, and the bubbles did not grow to visible sizes (Besra, Uchikoshi, Suzuki, & Sakka, 2010). Cross-sections of the CNF hydrogels showed that the interiors of the hydrogels deposited at 2.5 V tended to be uniform and oriented horizontally with respect to the anode surface (Fig. 4b, Fig. S3). On the other hand, the internal structures of the hydrogels prepared at 5 V and 10 V were disordered and showed nonuniform tendencies (Fig. 4d, f, Fig. S3). There are several possibilities for the changes occurring in the CNF orientations and hierarchical structures with applied voltage. Bubbles in the CNF hydrogels may be one factor; however, there was a report that the out-of-plane CNF orientation was changed by an applied voltage without bubbles (Kasuga et al., 2022). The hierarchical structures of the CNFs in a hydrogel is an important parameter for several applications, such as film preparation (Kasuga et al., 2022; Wilson et al., 2018), and further investigation of the underlying mechanism is needed.

3.5. Reuse of concentrated CNF hydrogels by electrodeposition

Finally, the reusabilities of concentrated CNF hydrogels were investigated. When a CNF hydrogel was simply diluted and homogenized (Fig. 5a), light transmittance of the dispersion was maintained at the original level (Fig. 5b). When large-scale CNF aggregates remained in the dispersion, the light transmittance of the dispersion decreased (Hsieh, Koga, Suganuma, & Nogi, 2017). This confirmed that after electrodeposition, the CNF hydrogel was redispersed to some extent by dilution and homogenization. CNF films were then prepared by drying the redispersed dispersion (Fig. 6a). The appearance of the prepared CNF film was clearly transparent (Fig. S4). The total transmittance of the

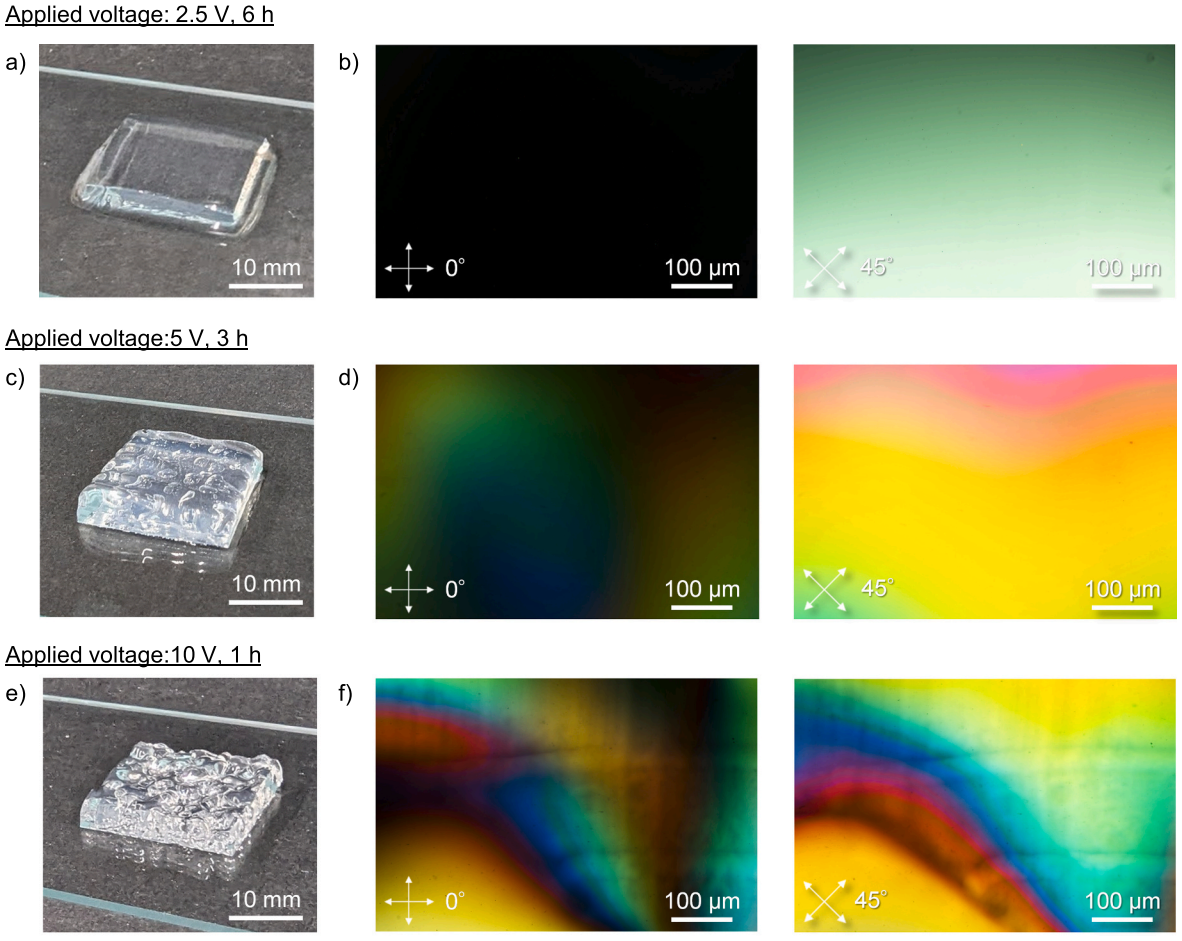

Fig. 4. CNF hydrogels formed by electrodeposition at applied voltages of a), b) 2.5 V, c), d) 5 V, and e), f) 10 V and cross-sectional polarized optical microscopy images.

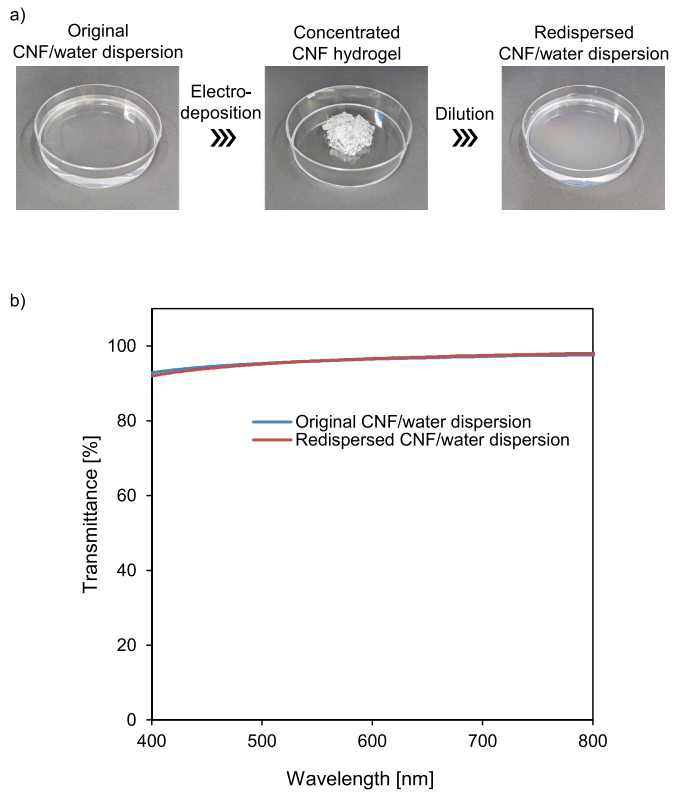

Fig. 5. a) Concentrated CNF hydrogels formed by electrodeposition were redispersed by a simple dilution and agitation process. b) The redispersed CNF/water dispersion exhibited almost the same transparency as the original dispersion.

dried CNF film prepared by drying of the redispersed CNF/water dispersion did not decrease (Fig. S5). However, the haze of the film increased, and the film became slightly translucent (Fig. 6b). The surface roughness of the CNF film was also higher than that of the original dispersion (Fig. 6c). The carboxylate groups on the surface of the deposited CNF hydrogels were protonated, and the CNFs formed a network structure (Saito, Uematsu, Kimura, Enomae, & Isogai, 2011). Therefore, simple dilution and homogenization of the CNF hydrogels may have left small CNF aggregates, resulting in the increased haze (Isobe et al., 2018; Kasuga et al., 2018). Neutralization was used to disintegrate the CNF aggregates. A 0.1 M sodium hydroxide solution was added to the CNF dispersion until the pH of the dispersion reached 7. As a result, the haze and surface roughness levels of the dried CNF films were returned to those of the original film (Fig. 6b, c). These results confirmed that the concentrated CNF hydrogel obtained by electrodeposition could be redispersed via a simple neutralization process.

4. Conclusion

Electrodeposition is a promising dehydration method for CNFs. For dilute CNF/water dispersions, dehydration by electrodeposition was much more efficient than evaporation. Interestingly, the hierarchical structures of the CNFs after electrodeposition varied with the applied voltage. In addition, the concentrated CNF hydrogels were reused with neutralization and homogenization processes, and clear, transparent films were prepared. In a limitation of electrodeposition, it was found that a long time was required to achieve a CNF/water dispersion with a concentration above 2 wt%. Further studies are needed to increase the concentration, such as by applying a higher voltage or changing the distance between electrodes according to the degree of dehydration. In the future, the effect of the type of CNFs also needs to be examine. While this method is effective for highly charged and nano-sized CNFs, such as

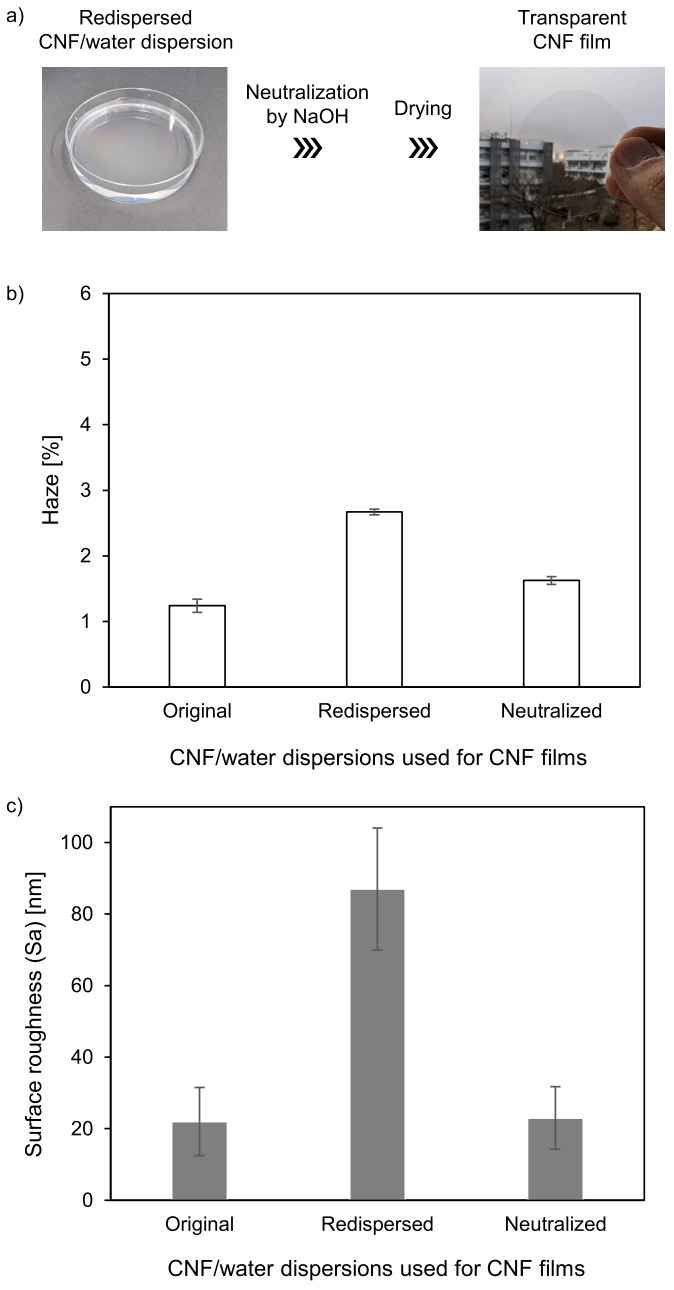

Fig. 6. a) CNF film preparation from a redispersed CNF/water dispersion. B) Haze and c) surface roughness of the CNF films prepared from the original, redispersed, and neutralized CNF/water dispersions.

TEMPO-oxidized CNFs, it might have limited effect on less charged and micro-sized cellulose fibers, such as microfibrillated cellulose (MFCs). These results provide new insights into dehydration via electrodeposition and the use of electrodeposition for hierarchical control of CNF structures.

CRediT authorship contribution statement

Takaaki Kasuga: Writing – review & editing, Writing – original draft, Visualization, Validation, Supervision, Resources, Project administration, Methodology, Investigation, Funding acquisition, Formal analysis, Data curation, Conceptualization. **Chenyang Li:** Investigation, Funding acquisition, Data curation. **Ami Mizui:** Resources, Data curation. **Shun Ishioka:** Investigation, Data curation. **Hirotaka Koga:** Writing – review & editing, Resources. **Masaya Nogi:** Writing – review

& editing, Resources, Funding acquisition.

Declaration of competing interest

The authors declare that they have no known competing financial interests or personal relationships that could have appeared to influence the work reported in this paper.

Data availability

Data will be made available on request.

Acknowledgments

This work was partially supported by Grants-in-Aid for Scientific Research (Grant Number JP22K20592, JP22KJ2188), JST ACT-X (Grant Number JPMJAX21K3), JST CREST (Grant Number JPMJCR22L3), and the Shorai Foundation for Science and Technology.

Appendix A. Supplementary data

Supplementary data to this article can be found online at https://doi.org/10.1016/j.carbpol.2024.122310.

References

Abe, K., Iwamoto, S., & Yano, H. (2007). Obtaining cellulose nanofibers with a uniform width of 15 nm from wood. *Biomacromolecules, 8*(10), 3276–3278.
Besra, L., Uchikoshi, T., Suzuki, T. S., & Sakka, Y. (2010). Experimental verification of pH localization mechanism of particle consolidation at the electrode/solution interface and its application to pulsed DC electrophoretic deposition (EPD). *Journal of the European Ceramic Society, 30*(5), 1187–1193.
Guccini, V., Yu, S., Agthe, M., Gordeyeva, K., Trushkina, Y., Fall, A., Schütz, C., & Salazar-Alvarez, G. (2018). Inducing nematic ordering of cellulose nanofibers using osmotic dehydration. *Nanoscale, 10*(48), 23157–23163.
Guo, X., Gao, H., Zhang, J., Zhang, L., Shi, X., & Du, Y. (2020). One-step electrochemically induced counterion exchange to construct free-standing carboxylated cellulose nanofiber/metal composite hydrogels. *Carbohydrate Polymers, 117464*.
Hsieh, M. C., Koga, H., Suganuma, K., & Nogi, M. (2017). Hazy transparent cellulose nanopaper. *Scientific Reports, 7*(1), 1–7.
Huang, Y., Kasuga, T., Nogi, M., & Koga, H. (2023). Clearly transparent and air-permeable nanopaper with porous structures consisting of TEMPO-oxidized cellulose nanofibers. *RSC Advances, 13*(31), 21494–21501.
Isobe, N., Kasuga, T., & Nogi, M. (2018). Clear transparent cellulose nanopaper prepared from a concentrated dispersion by high-humidity drying. *RSC Advances, 8*(4), 1833–1837.
Isogai, A., Saito, T., & Fukuzumi, H. (2011). TEMPO-oxidized cellulose nanofibers. *Nanoscale, 3*(1), 71–85.
Karna, N. K., Lidén, A., Wohlert, J., & Theliander, H. (2021). Electroassisted filtration of microfibrillated cellulose: Insights gained from experimental and simulation studies. *Industrial and Engineering Chemistry Research, 60*(48), 17663–17676.
Kasuga, T., Isobe, N., Yagyu, H., Koga, H., & Nogi, M. (2018). Clearly transparent nanopaper from highly concentrated cellulose nanofiber dispersion using dilution and sonication. *Nanomaterials, 8*(2), 104.
Kasuga, T., Mizui, A., Koga, H., & Nogi, M. (2023). Wirelessly powered sensing fertilizer for precision and sustainable agriculture. *Advanced Sustainable Systems, 2300314*.
Kasuga, T., Saito, T., Koga, H., & Nogi, M. (2022). One-pot hierarchical structuring of nanocellulose by electrophoretic deposition. *ACS Nano, 16*(11), 18390–18397.
Kasuga, T., Yagyu, H., Uetani, K., Koga, H., & Nogi, M. (2019). "Return to the soil" nanopaper sensor device for hyperdense sensor networks. *ACS Applied Materials and Interfaces, 11*(46), 43488–43493.
Kasuga, T., Yagyu, H., Uetani, K., Koga, H., & Nogi, M. (2021). Cellulose nanofiber coatings on cu electrodes for cohesive protection against water-induced short-circuit failures. *ACS Applied Nano Materials, 12*, 41.
Kim, H., Endrődi, B., Salazar-Alvarez, G., & Cornell, A. (2019). One-step electro-precipitation of nanocellulose hydrogels on conducting substrates and its possible applications: Coatings, composites, and energy devices. *ACS Sustainable Chemistry and Engineering, 7*(24), 19415–19425.
Lasseuguette, E., Roux, D., & Nishiyama, Y. (2008). Rheological properties of microfibrillar suspension of TEMPO-oxidized pulp. *Cellulose, 15*(3), 425–433.
Li, C., Kasuga, T., Uetani, K., Koga, H., & Nogi, M. (2020). High-speed fabrication of clear transparent cellulose Nanopaper by applying humidity-controlled multi-stage drying method. *Nanomaterials, 10*(11), 2194.
Li, Q., Hatakeyama, M., & Kitaoka, T. (2022). Bioadaptive porous 3D scaffolds comprising cellulose and chitosan nanofibers constructed by Pickering emulsion templating. *Advanced Functional Materials, 32*(22), 2200249.
Nemoto, J., Saito, T., & Isogai, A. (2015). Simple freeze-drying procedure for producing nanocellulose aerogel-containing, high-performance air filters. *ACS Applied Materials and Interfaces, 7*(35), 19809–19815.
Saito, T., Uematsu, T., Kimura, S., Enomae, T., & Isogai, A. (2011). Self-aligned integration of native cellulose nanofibrils towards producing diverse bulk materials. *Soft Matter, 7*(19), 8804–8809.
Sakuma, W., Fujisawa, S., Berglund, L. A., & Saito, T. (2021). Nanocellulose xerogel as template for transparent, thick, flame-retardant polymer nanocomposites. *Nanomaterials, 11*(11), 3032.
Sakuma, W., Yamasaki, S., Fujisawa, S., Kodama, T., Shiomi, J., Kanamori, K., & Saito, T. (2021). Mechanically strong, scalable, mesoporous xerogels of nanocellulose featuring light permeability, thermal insulation, and flame self-extinction. *ACS Nano, 15*(1), 1436–1444.
Sekine, Y., Nankawa, T., Yunoki, S., Sugita, T., Nakagawa, H., & Yamada, T. (2020). Eco-friendly carboxymethyl cellulose nanofiber hydrogels prepared via freeze cross-linking and their applications. *ACS Applied Polymer Materials, 2*(12), 5482–5491.
Sheng, J., & Yang, R. (2019). A facile method to concentrate cellulose nanofibril slurries. *Cellulose, 26*(2), 679–682.
Shimizu, M., Saito, T., & Isogai, A. (2016). Water-resistant and high oxygen-barrier nanocellulose films with interfibrillar cross-linkages formed through multivalent metal ions. *Journal of Membrane Science, 500*, 1–7.
Sinquefield, S., Ciesielski, P. N., Li, K., Gardner, D. J., & Ozcan, S. (2020). Nanocellulose dewatering and drying: Current state and future perspectives. *ACS Sustainable Chemistry and Engineering, 8*(26), 9601–9615.
Sone, A., Saito, T., & Isogai, A. (2016). Preparation of aqueous dispersions of TEMPO-oxidized cellulose nanofibrils with various metal counterions and their super deodorant performances. *ACS Macro Letters, 5*(12), 1402–1405.
Wetterling, J., Sahlin, K., Mattsson, T., Westman, G., & Theliander, H. (2018). Electroosmotic dewatering of cellulose nanocrystals. *Cellulose, 25*(4), 2321–2329.
Wilson, B. P., Yliniemi, K., Gestranius, M., Hakalahti, M., Putkonen, M., Lundström, M., … Kontturi, E. (2018). Structural distinction due to deposition method in ultrathin films of cellulose nanofibres. *Cellulose, 25*(3), 1715–1724.
Yagyu, H., Kasuga, T., Ogata, N., Koga, H., Daicho, K., Goi, Y., … Goi, Y. (2023). Evaporative dry powders derived from cellulose nanofiber organogels to fully recover inherent high viscosity and high transparency of water dispersion. *Macromolecular Rapid Communications, 44*(17), 2300186.
Yang, X., Reid, M. S., Olsén, P., & Berglund, L. A. (2020). Eco-friendly cellulose nanofibrils designed by nature: Effects from preserving native state. *ACS Nano, 14*(1), 724–735.
Zhai, L., Kim, H. C., Kim, J. W., & Kim, J. (2020). Simple centrifugal fractionation to reduce the size distribution of cellulose nanofibers. *Scientific Reports, 10*(1), 1–8.
Zhao, M., Ansari, F., Takeuchi, M., Shimizu, M., Saito, T., Berglund, L. A., & Isogai, A. (2017). Nematic structuring of transparent and multifunctional nanocellulose papers. *Nanoscale Horizons, 3*(1), 28–34.
Zhu, L., Li, X., Kasuga, T., Uetani, K., Nogi, M., & Koga, H. (2022). All-cellulose-derived humidity sensor prepared via direct laser writing of conductive and moisture-stable electrodes on TEMPO-oxidized cellulose paper. *Journal of Materials Chemistry C, 10*(10), 3712–3719.